

Research Article

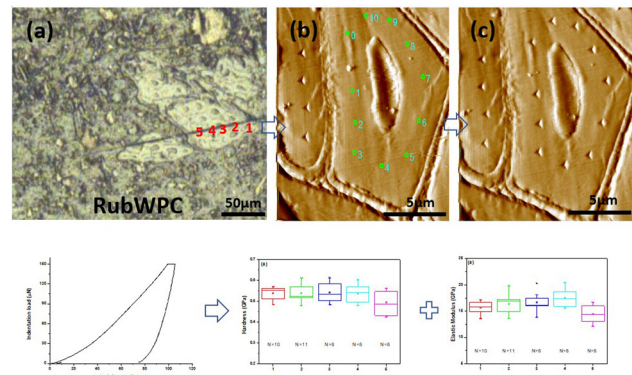
Yonghui Zhou, David Hui, Yuxuan Wang, and Mizi Fan*

Nanomechanical and dynamic mechanical properties of rubber–wood–plastic composites

<https://doi.org/10.1515/ntrev-2022-0002>
received July 10, 2021; accepted August 21, 2021

Abstract: This article presents the assessment of bulk and *in situ* mechanical properties of rubber–wood–plastic composites (RubWPC) and their correlations, aiming to obtain a thorough understanding of mechanical behaviour of RubWPC, which is an essential prerequisite in realising their optimal design and applications. Dynamic mechanical analysis results showed that the composites treated with multiple coupling agents (combination of maleic anhydride polyethylene [MAPE] and bis(triethoxysilylpropyl) tetrasulfide and combination of MAPE and vinyltrimethoxysilane) exhibited greater storage modulus than both the untreated and single coupling agent treated composites owing to their superior interfacial bonding quality. The shift of relaxation peak and T_g towards higher temperatures observed in the treated composites confirmed the enhancement of interfacial interaction and adhesion. Nanoindentation analysis suggested that the composite with optimised interface (MAPE and Si69 treated) possessed better nanomechanical property (elastic modulus) due to the resin penetration into cell lumens and vessels and the reaction between cell walls and coupling agents.

Keywords: rubber–wood–plastic composites, nanoindentation, nanomechanical, dynamic mechanical analysis



Graphical abstract

1 Introduction

The ever-increasing environmental concerns towards the global disposal of waste tyres has led to an unprecedented need to recycle and reuse the main component of the tyres, namely tyre rubber [1,2]. Currently, the incorporation of waste tyre rubber into thermoplastics to develop a class of polymer composites with both elastomeric and thermoplastic behaviour has gained a lot of attention and is becoming one of the most straightforward and preferred options to achieve the valorisation of waste tyres [3,4]. In view of the unique properties possessed by rubber and the rapid expansion and versatile application of wood plastic composite (WPC) materials, the inclusion of tyre rubber as a raw material into WPC to develop an entirely new generation of WPC, namely rubber–wood–plastic composites (RubWPC), was presumed to be another highly promising solution to turn waste tyres into value-added materials. Cosnita *et al.* investigated multifunctional, environmental-friendly composite materials fully based on wastes of polyethylene terephthalate (PET), rubber, high density polyethylene (HDPE), and wood, aiming for indoor and outdoor applications [5]. The work particularly addressed the limited rubber-PET compatibility with the aid of HDPE, so as to obtain good mechanical and stability properties. Moni Ribeiro Filho *et al.* developed hybrid composites with epoxy polymer,

* **Corresponding author: Mizi Fan**, Department of Civil and Environmental Engineering, Brunel University London, UB8 3PH, Uxbridge, United Kingdom, e-mail: mizi.fan@brunel.ac.uk

Yonghui Zhou, Yuxuan Wang: Department of Civil and Environmental Engineering, Brunel University London, UB8 3PH, Uxbridge, United Kingdom

David Hui: Department of Mechanical Engineering, University of New Orleans, Lake Front, New Orleans, LA 70138, United States of America

rubber tyre particles, and sugarcane bagasse fibres with a specific focus on the impact behaviour [6]. It was concluded that in general, the combination of rubber wastes and bagasse fibres appeared to offer an appealing alternative for the development of new sustainable structural materials for low-carbon impact engineering applications.

Thorough understanding of mechanical properties of composites is an essential prerequisite in realising their applications [7]. The major factors affecting the mechanical performance of cellulosic polymer composites include: (1) the strength and modulus of reinforcing fibre, (2) the strength and chemical stability of polymer matrix, and (3) the effectiveness of load transfer across interface [8]. Investigation of interface is of special significance in understanding the macro-behaviour of the composites [9,10]. Interface is the region separating the bulk polymer from the fibrous reinforcement. It is not a distinct phase with clear boundaries, it is more accurately viewed as a transition zone with three-dimensional and heterogeneous nature. Interface region is hypothesised to possess mechanical properties distinct from those of the reinforcing phase and bulk polymer [11]. Recently, the direct determination of the property and size of interface of cellulosic polymer composites has been achieved with the advent of depth sensing indentation technique, which is generally referred to as nanoindentation [12,13]. This technique allows the penetration of an indenter into the material surface with controlled force and synchronous recording of the force applied as a function of indentation depth, and thus provides considerable *in situ* mechanical property information (*e.g.* elastic modulus, hardness, and creep factor) [14,15].

Following our report on the novel formulation of RubWPC with the focus on their interfacial optimisation by using maleated and silane coupling agents [16], and finding that the coupling agents could dramatically improve the constituent compatibility, filler dispersion and embedment, and interfacial adhesion of the composites, this work specifically investigates the nanomechanical and dynamic mechanical properties of RubWPC, aiming to understand the contribution of the refined interfacial bonding to the bulk and *in situ* mechanical properties

and their correlation, thus enabling the optimal design of RubWPC materials.

2 Materials and methods

2.1 Materials

The recycled tyre rubber used in this research was supplied by J. Allcock & Sons Ltd (UK), with the particle size between 0.05 and 0.5 mm and bulk density of 360 kg/m³. The recycled wood-flour was supplied by Rettenmeier Holding AG (Germany), with the bulk density of 285 kg/m³ and mean length of 0.55 mm. The recycled HDPE pellet with the melt flow index (MFI) of 0.6 g/10 min at 190°C and bulk density of 960 kg/m³ was obtained from JFC Plastics Ltd (UK).

Lubricants 12-hydroxyoctadecanoic acid (12-HSA) and Struktol TPW 709 (a unique proprietary blend of processing aids made by Struktol company) were purchased from Safic Alcan UK Ltd (Warrington, UK). The coupling agents, maleic anhydride polyethylene (MAPE, MFI of 1.9 g/10 min at 190°C, 0.5 wt% maleic anhydride [MA]), bis(triethoxysilylpropyl)tetrasulfide (Si69, >95% purity, 538.95 g/mol, 250°C boiling point), and vinyltrimethoxysilane (VTMS, >98% purity, 148.23 g/mol, 123°C boiling point), were purchased from Sigma-Aldrich (Dorset, UK), the chemical formulae of which are presented in Figure 1. All the raw materials and additives were stored in a cool and dry place before use.

2.2 Formulation of RubWPC

The formulation of untreated and treated RubWPC with specific ratios was summarised in Table 1. In our previous works [3,17], it was found that VTMS and Si69 were very effective in improving the bonding quality of WPC and Rubber-HDPE composites, respectively, while MAPE appeared to be effective in both types of materials.

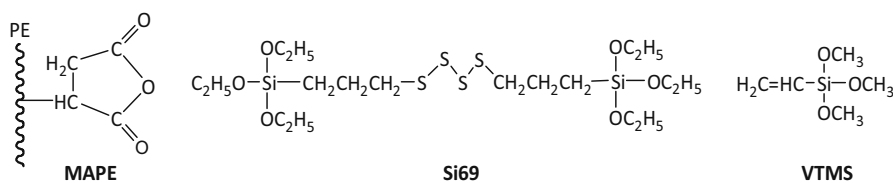


Figure 1: Chemical formulae of the coupling agents.

Table 1: Formulation of RubWPC

Sample	Rubber (%)	Wood (%)	HDPE (%)	TPW 709 (%)	12HSA (%)	MAPE (%)	Si69 (%)	VTMS (%)
Untreated	20	30	43	3.5	3.5	0	0	0
MAPE treated	20	30	40	3.5	3.5	3	0	0
Si69 treated	20	30	40	3.5	3.5	0	3	0
VTMS treated	20	30	40	3.5	3.5	0	0	3
MAPE and Si69	20	30	40	3.5	3.5	1.5	1.5	0
MAPE and VTMS	20	30	40	3.5	3.5	1.5	0	1.5
MAPE and Si69-10	10	40	40	3.5	3.5	1.5	1.5	0
MAPE and Si69-30	30	30	30	3.5	3.5	1.5	1.5	0

Therefore, in addition to single coupling agent, the combinations of MAPE and Si69 and MAPE and VTMS were also used in the formulation of RubWPC materials. All the composites were prepared under the processing condition as follows: the required amount of HDPE for each batch was first placed in a Brabender Plastograph twin-screw mixer and allowed to melt at 100 rpm and 190°C for 2 min, and subsequently mixed with rubber powder and wood flour for 3 min. The lubricants and/or coupling agents were then added into the system and mixed for another 10 min. The resulted RubWPC mixture was then ground to pellets by using a Retsch cutting mill (SM 100, Germany). The ground blends were compression moulded on an electrically heated hydraulic press at 190°C under a pressure of 9.81 MPa for 10 min.

2.3 Dynamic mechanical analysis (DMA)

Dynamic mechanical properties of the composites were measured by using a dynamic mechanical analyser (Q800, TA Instruments, New Castle, USA) under single cantilever

strain-controlled mode. The temperature ranges from -100 to 120°C with a heating rate of 3°C/min. The oscillation amplitude was 20 µm, the frequency was 1 Hz, and the specimen dimension was 17.5 mm × 10.8 mm × 1.4 mm.

2.4 Nanoindentation analysis

The samples for nanoindentation determination were prepared as follows: a sloping apex (around 45°) was created on the cross section of the sample by using a sliding microtome, then the sample was mounted onto a PowerTome ultramicrotome and transversely cut with a glass knife and a diamond knife to obtain an exceptionally smooth and flat surface. The cross section of the samples was first observed under an optical microscope to select the regions to be indented (Figure 2a). The tests were performed on a Nano Indenter (Hysitron TI 950 TriboIndenter, USA) equipped with a three-side pyramid diamond indenter tip (Berkovich). In each test region, the space between two adjacent testing positions was 30 times more than the maximum indentation depth

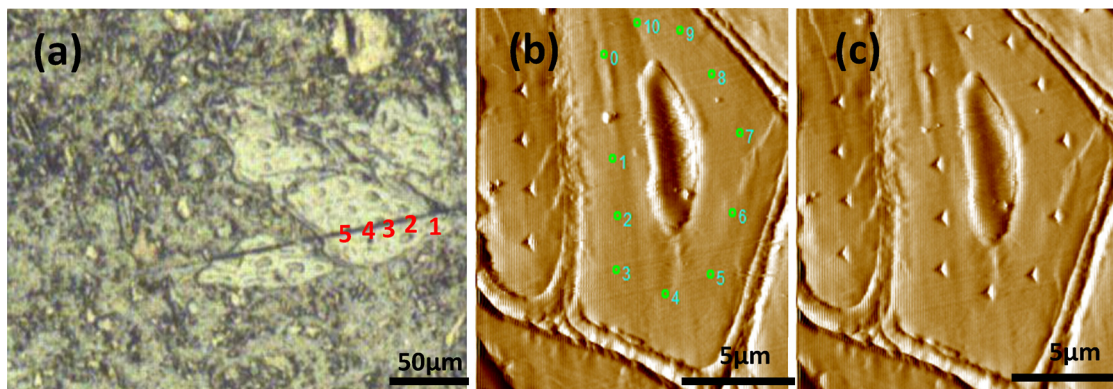


Figure 2: Typical *in situ* imaging nanoindentation test: (a) microscope image of testing cells in transverse section, (b) image of cell walls in region 1 of (a) before indenting, and (c) image of cell walls in region 1 of (a) after indenting.

(Figure 2b and c). The indentations were conducted under load-controlled mode consisting of three segments, *i.e.* loading with 150 μN in 5 s, holding for 2 s, and unloading in 5 s. A typical loading-displacement curve is presented in Figure 3. The maximum load P_{\max} , the maximum depth h_{\max} , the final depth after unloading h_r , and the slope of the upper portion of the unloading curve S were monitored in a full loading-unloading cycle. The material properties, such as reduced elastic modulus and hardness, could be extracted by analysing the data with the method developed by Oliver and Pharr [18].

The hardness (H) was calculated as follows:

$$H = \frac{P_{\max}}{A}, \quad (1)$$

where A is the projected contact area at maximum load. E_r , the reduced elastic modulus accounting for the compliance of the indenter tip, was determined as:

$$E_r = \frac{\sqrt{\pi}}{2} \frac{dP}{dh} \frac{1}{\sqrt{A}}, \quad (2)$$

where, $dP/dh = S$. The results reported in the work were from the indentations placed in the valid positions, clearly on the cells with intimate and firm resin contact, excluding the results from cracks and other positions.

3 Results and discussion

3.1 The DMA

The transition of a polymeric material from glassy state to rubbery state, commonly investigated by DMA, has been

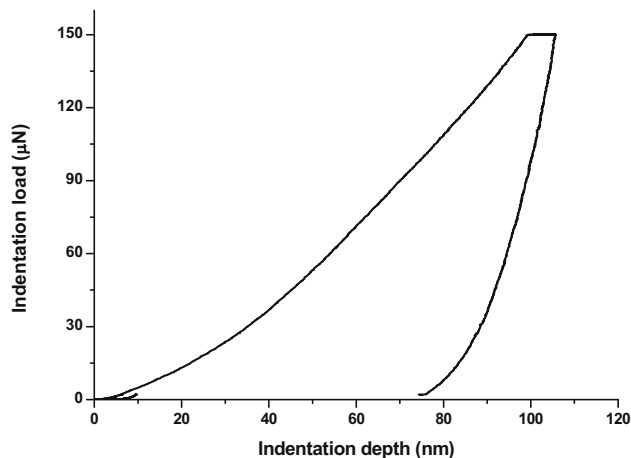


Figure 3: Typical loading-unloading curve of nanoindentation test.

considered as a significant material property. Figure 4 illustrates the temperature dependence of the storage moduli of both the untreated and coupling agent treated RubWPC. The storage moduli of all the composites gradually decreased with the increase in temperature. Compared to the untreated counterpart, the composites treated with single coupling agent (*i.e.* MAPE, Si69, or VTMS) showed inferior storage moduli in the temperature range from -100 to -50°C . At the temperature above -50°C , the storage moduli of MAPE and Si69 treated composites were higher than that of the untreated composites, while that of VTMS-treated composites remained slightly lower, but appeared to be much closer. In our previous studies of WPC [19] and rubber-HDPE composites [3], the use of single coupling agent was able to enhance the storage modulus of the composites. The distinct phenomena observed in RubWPC could be ascribed to the uneven distribution of coupling agent between the fillers (wood flour and rubber powder) in the complex RubWPC system, which resulted in relatively nonuniform and heterogeneous structures and poor overall bonding refinery. Furthermore, it was worth noting that the composites treated with combined coupling agents, especially MAPE and VTMS, exhibited greater modulus values than both untreated and single coupling agent treated composites. Compared to single coupling agent, the combination of MAPE and Si69 or MAPE and VTMS might generate a complementary influence, maximising the capability of interface refining and bonding strengthening of each coupling agent. This result was in accordance with the tensile properties owing to the superior interfacial adhesion and bonding quality, which had been revealed in our previous study [16].

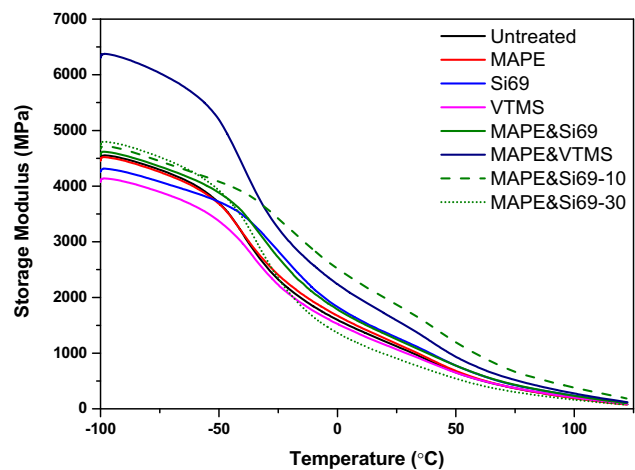


Figure 4: Storage modulus of untreated and coupling agent treated RubWPC as a function of temperature.

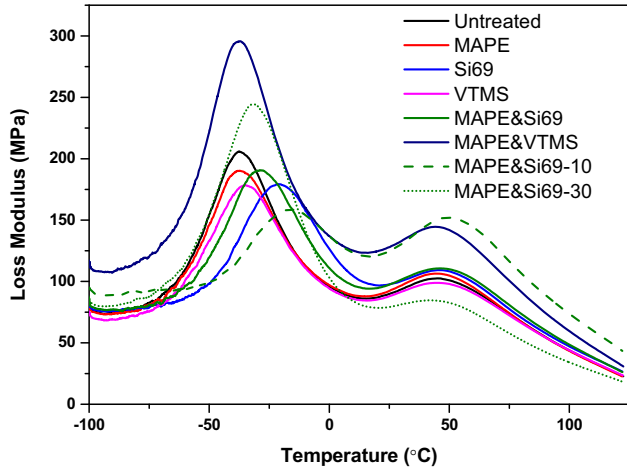


Figure 5: Loss modulus of untreated and coupling agent treated RubWPC as a function of temperature.

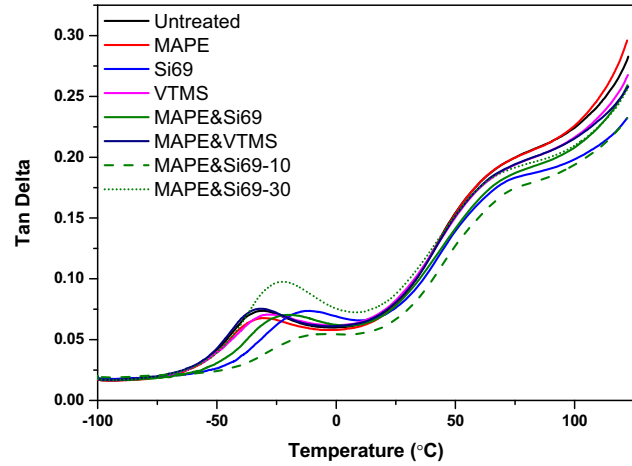


Figure 6: $\tan \delta$ of untreated and coupling agent treated RubWPC as a function of temperature.

The loss modulus is a measure of the energy dissipated as heat, representing the viscous portion of the material that flows under certain condition of stress. Figure 5 presents the variation in loss modulus as a function of temperature of the composites. The relaxation peaks at -38 to -16°C in the curves were associated with the molecular motion of rubber phase corresponding to its glass transition (Table 2). It was observed that the coupling agent treatments led to a flattening of the relaxation peaks with lowered loss modulus values, and a shift of relaxation peaks from -38.0°C (untreated) towards higher temperatures (Table 2). These results indicated the enhanced interfacial interaction and adhesion between rubber particles and other constituents of the composites. In addition, the relaxation peaks observed at around 50°C were attributed to the α transition of HDPE matrix, corresponding to its chain segment mobility [20–22]. The relevant loss modulus at this temperature was seen to have a marginal increase after the coupling agent treatments, which was probably due to the reduced flexibility by introducing constraints on

the segmental mobility of macromolecules at the relaxation temperatures [23,24].

The damping property of material gives a balance between the elastic phase and viscous phase in a polymeric structure. The mechanical loss factor or damping factor $\tan \delta$ of the composites as a function of temperature is presented in Figure 6. The glass transition temperatures (T_g) of the treated composites shifted to higher temperatures, namely from -33.2°C (untreated) to -32.3°C (MAPE treated), -13.0°C (Si69 treated), -29.3°C (VTMS treated), -21.7°C (MAPE and Si69 treated), and -32.8°C (MAPE and VTMS treated), (Table 2). This observation should be associated with the intermolecular crosslinking induced by the coupling agent treatments [25], which had been thoroughly discussed in our previous work (16), *i.e.* the hydrophilic moieties in coupling agents (maleic anhydride of MAPE, ethoxy groups of Si69, and methoxyl groups of VTMS) reacted with the hydroxyl groups of wood flour to form strong covalent bonds, while the non-polar molecules (PE chains in MAPE, dissociated sulfide

Table 2: Crucial parameters extracted from DMA curves of RubWPC

Sample	Temperature of rubber relaxation peak [T_r] ($^\circ\text{C}$)	Loss modulus at T_r (MPa)	Glass transition temperature [T_g] ($^\circ\text{C}$)	$\tan \delta$ at T_g
Untreated	-38.0	205.7	-33.2	0.073
MAPE treated	-37.5	190.1	-32.3	0.067
Si69 treated	-20.5	179.1	-13.0	0.073
VTMS treated	-34.8	178.6	-29.3	0.071
MAPE and Si69	-28.9	190.5	-21.7	0.070
MAPE and VTMS	-37.5	295.6	-32.8	0.075
MAPE and Si69-10	-16.4	158.5	-9.1	0.054
MAPE and Si69-30	-31.7	244.5	-22.5	0.098

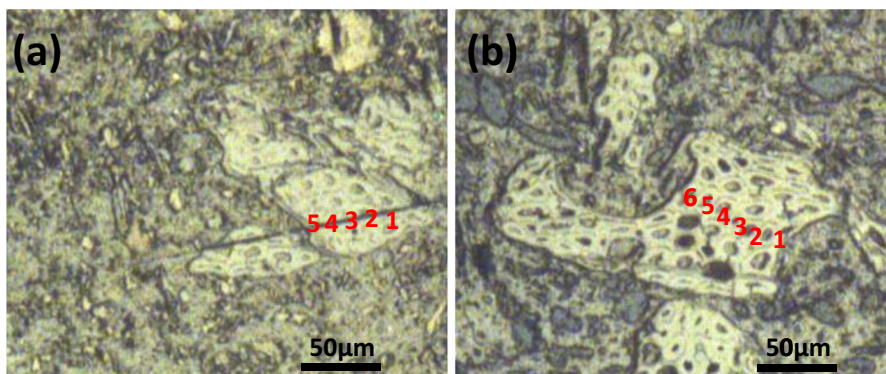


Figure 7: Microscope images of nanoindentation test regions of untreated (a) and MAPE and Si69 treated (b) RubWPC.

groups of Si69, and vinyl groups of VTMS) chemically crosslinked with rubber and HDPE macromolecules. The presence of the crosslinking was assumed to restrict the mobility of the polymeric chains so that more energy was required for the transition to occur [26]. On the other hand, the decline in the $\tan \delta$ intensity or amplitude of the treated composites (Table 2) suggested that the number of molecular portions responsible for the transitions had decreased after the treatments [26]. This result along with their better interfacial bonding, reduced interchain chemical heterogeneity, and relatively restricted segmental mobility of polymer molecules gave rise to less energy dissipation in the treated composites, leading to the reduction in the $\tan \delta$ amplitude.

As presented in Table 2, Si69 and MAPE and Si69 treated composites had much higher glass transition temperatures, compared to other composites. This was because Si69 has proven to be a highly effective coupling agent for enhancing bonding quality of rubber based composites [27–30], and it could significantly improve the interfacial bonding and molecular interactions between rubber and HDPE, resulting in greater immobility of molecular chains. However, the Si69 added in Si69-treated RubWPC could be primarily dominated by rubber particles which favourably reacted with HDPE molecules. Due to this, the bonding between wood flour and other components (rubber and HDPE) in the composite could hardly be improved without the presence of MAPE, which thus impaired its overall property.

It was seen that a gradual decrease in the storage modulus with the continuous addition of rubber into MAPE and Si69 treated composites, indicates the decrease in stiffness of the composites. Regarding the difference between the composites with 20 and 30% rubber, the lower storage modulus in the composite with 30% rubber was ascribed to its poorer filler distribution and wetting due to the lower concentration of HDPE matrix in the system. The relaxation

peaks of the composites with less rubber addition were observed at higher temperature regions, which were consistent with their higher T_g . This suggests that the stronger rubber-wood and rubber-HDPE interactions occurred in the composites contributed to the segmental immobilisation

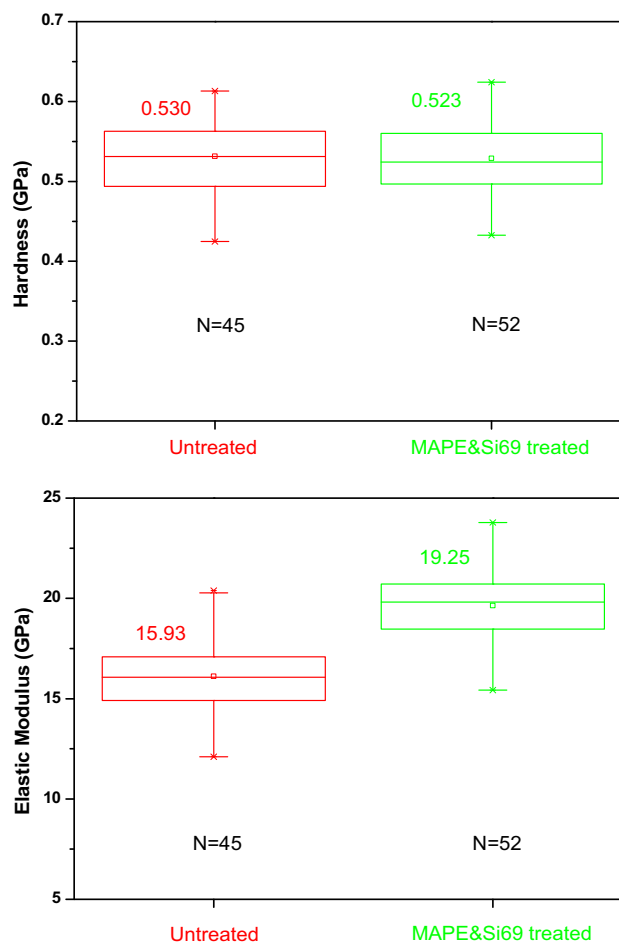


Figure 8: Nanomechanical properties of untreated and MAPE and Si69 treated RubWPC by nanoindentation.

of the polymer chain along the interfaces and hence, caused a lowering of the corresponding $\tan \delta$ amplitude [31].

3.2 Nanomechanical property analysis

Figure 7 shows the nanoindentation test regions of untreated and MAPE and Si69 treated RubWPC, the results from the measurements are presented in Figure 8. The hardness of the cell walls in the treated composite was nearly equal to that of untreated composite. In contrast, the reduced elastic modulus of the treated cell walls was significantly increased by 20.84% compared to that of untreated cell walls, which was well in line with its storage modulus (Figure 4). This result might be associated with the considerable penetration of polymer resin into the more deformed and accessible cell lumens and vessels after the treatment [16]. Although it was widely accepted that the indentation modulus in damaged

cell walls were lower than that in intact cell walls, the resin filling in cell lumens may work as a mechanical interlock that could provide additional strength, recovering the loss of elastic behaviour due to mechanical processing [32–34]. It was worth mentioning that in our previous nanoindentation analysis of WPC [19], the coupling agent treatment might exert a weakening or softening impact on the cell walls through chain scission or weakening of interfibrillar interaction, resulting in lower mechanical properties compared to the untreated cell walls. The contrary behaviour explored in RubWPC indicated that with respect to the influence on nanomechanical properties of treated cell walls, the resin penetration was more pronounced over the weakening or softening impact with the inclusion of rubber particles into the composite. Therefore, the nanomechanical properties of the cell walls in untreated RubWPC remained unaffected by the rubber particles due to the lack of intimate physical contact between wood flour and rubber particle in untreated

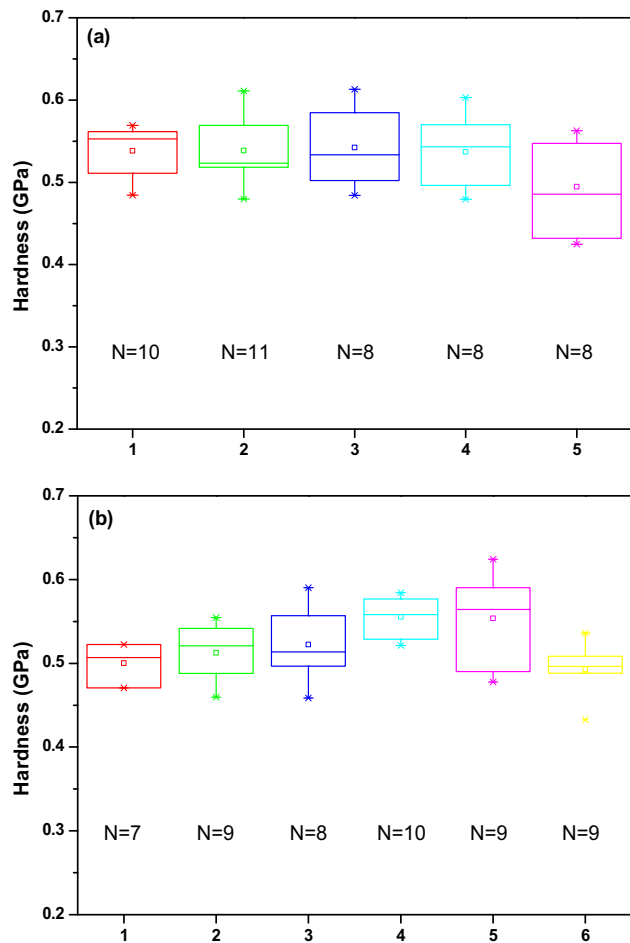


Figure 9: Comparison of the hardness in different test regions of untreated (a) and MAPE and Si69 treated (b) RubWPC.

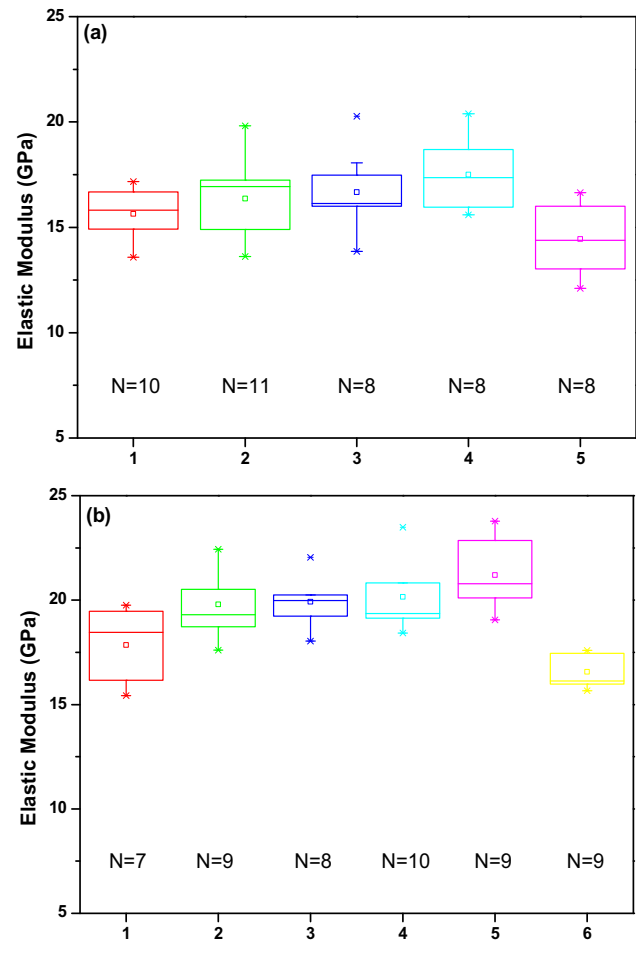


Figure 10: Comparison of the reduced elastic modulus in different test regions of untreated (a) and MAPE and Si69 treated (b) RubWPC.

RubWPC [16], leading to subtle distinction from the nanomechanical properties of WPC [19]. In addition, MAPE and Si69 coupling agents might be able to diffuse into wood cell wall and form hydrogen bonding and covalent bonding with the structural components of the cell wall especially hemicellulose owing to its greater accessibility [33], thus increasing the nanomechanical property of the treated RubWPC.

The individual nanomechanical property of every marked region in Figure 7 is presented in Figures 9 and 10 for the purpose of figuring out the variation in the nanomechanical behaviour of the cell walls. The hardness and indentation modulus of the cell wall in both untreated and MAPE and Si69 treated composites increased with the increase in its distance to the zone being in immediate contact with rubber particle and HDPE matrix. For instance, the elastic moduli in region 1 (15.64 GPa) and region 5 (14.45 GPa) were lower than those in region 3 (16.67 GPa) and region 4 (17.50 GPa) of the untreated composite, the hardness in region 1 or region 6 of the treated composite was not comparable to the counterpart in other regions. This was because the cell wall in intimate contact with other components was more deformed than the cell wall further away from the bonding region, leading to inferior local mechanical property [34], albeit it might have more resin penetration into the adjacent cell lumen and coupling agent diffusion. Furthermore, the hardness or modulus distinction among different regions of the untreated composite (up to 0.05 and 3.05 GPa, respectively) was not as apparent as that of the treated composite (up to 0.06 GPa and 4.64 GPa, respectively) due to the less deformed and accessible cell walls in the untreated composite, which was in accordance with their microstructure [16].

4 Conclusion

The assessment of bulk and *in situ* mechanical properties of untreated and coupling agent treated RubWPC was accomplished by systematically carrying out DMA and nanoindentation measurements. The enhanced interfacial bonding of the treated RubWPC was confirmed by the shift of relaxation peak and T_g towards higher temperatures along with the reduction in $\tan \delta$ amplitude, which were associated with the restricted segmental polymer motion and less energy dissipation. The composites with less rubber addition demonstrated the corresponding relaxation peaks at higher temperatures with higher T_g and lower $\tan \delta$ amplitude, primarily due to their stronger interfacial interactions. The composites treated

with multiple coupling agents (MAPE and Si69 or MAPE and VTMS) exhibited better overall mechanical properties than the composites treated with single coupling agent owing to their superior interfacial bonding. MAPE and Si69 treated RubWPC possessed more outstanding nanomechanical property than the untreated counterpart (*i.e.* elastic modulus increased from 15.93 to 19.25 GPa), which was ascribed to the considerable resin penetration into the more deformed and accessible cell lumens and vessels as well as the bonding formed between the diffused coupling agents and the structural components of cell walls. In addition, the nanomechanical properties (hardness and elastic modulus) of the cell wall in both untreated and treated composites increased with the increase in its distance to the interfacial zones being in intimate contact with rubber particle and HDPE matrix.

Funding information: This work was supported by European CIP-EIP-Eco-Innovation-2012 (Project number: 333083) and Horizon 2020 research and innovation programme (Project number: 869898, POWERSKIN PLUS).

Author contributions: Y.Z.: conceptualisation, investigation, and writing – original draft; Y.W. and D.H.: visualisation and validation; M.F.: supervision and writing – review & editing. All authors have accepted responsibility for the entire content of this article and approved its submission.

Conflict of interest: David Hui, who is the co-author of this article, is a current Editorial Board member of *Nanotechnology Reviews*. This fact did not affect the peer-review process. The authors declare no other conflict of interest.

References

- [1] Formela K, Hejna A, Zedler Ł, Przybysz M, Ryl J, Saeb MR, et al. Structural, thermal and physico-mechanical properties of polyurethane/brewers' spent grain composite foams modified with ground tire rubber. *Ind Crop Products*. 1 December 2017;108:844–52.
- [2] Zhao J, Wang X-, Chang JM, Yao Y, Cui Q. Sound insulation property of wood-waste tire rubber composite. *Compos Sci Technol*. 30 November 2010;70(14):2033–8.
- [3] Zhou Y, Fan M. Recycled tyre rubber-thermoplastic composites through interface optimisation. *RSC Adv*. 2017;7(47):29263–70.
- [4] Ramarad S, Khalid M, Ratnam CT, Chuah AL, Rashmi W. Waste tire rubber in polymer blends: A review on the evolution, properties and future. *Prog Mater Sci*. July 2015;72(72):100–40.

- [5] Cosnita M, Cazan C, Duta A. The influence of inorganic additive on the water stability and mechanical properties of recycled rubber, polyethylene terephthalate, high density polyethylene and wood composites. *J Clean Prod.* 1 November 2017;165:630–6.
- [6] Moni Ribeiro Filho SL, Oliveira PR, Panzera TH, Scarpa F. Impact of hybrid composites based on rubber tyre particles and sugarcane bagasse fibres. *Compos Part B: Eng.* 15 February 2019;159:157–64.
- [7] Alhijazi M, Zeeshan Q, Qin Z, Safaei B, Asmael M. Finite element analysis of natural fibers composites: a review. *Nanotechnol Rev.* 2020;9(1):853–75.
- [8] Kumar R, Cross WM, Kjerengtroen L, Kellar JJ. Fiber bias in nanoindentation of polymer matrix composites. *Composite Interfaces.* 2004 01/01;11(5–6):431–40.
- [9] Zhang T, Bai SL, Zhang YF, Thibaut B. Viscoelastic properties of wood materials characterized by nanoindentation experiments. *Wood Sci Technol.* 2012;46(5):1003–16.
- [10] Liu Y, Jiang X, Shi J, Luo Y, Tang Y, Wu Q, et al. Research on the interface properties and strengthening–toughening mechanism of nanocarbon-toughened ceramic matrix composites. *Nanotechnol Rev.* 2020;9(1):190–208.
- [11] Downing TD, Kumar R, Cross WM, Kjerengtroen L, Kellar JJ. Determining the interphase thickness and properties in polymer matrix composites using phase imaging atomic force microscopy and nanoindentation. *J Adhes Sci Technol.* 2000 01/01;14(14):1801–12.
- [12] Ganser C, Hirn U, Rohm S, Schennach R, Teichert C. AFM nanoindentation of pulp fibers and thin cellulose films at varying relative humidity. *Holzforschung.* 2013;68(1):53–60.
- [13] Zare Ghomsheh M, Spieckermann F, Polt G, Wilhelm H, Zehetbauer M. Analysis of strain bursts during nanoindentation creep of high-density polyethylene. *Polym Int.* 2015;64(11):1537–43.
- [14] Yedla SB, Kalukanimuttam M, Winter RM, Khanna SK. Effect of shape of the tip in determining interphase properties in fiber reinforced plastic composites using nanoindentation. *J Eng Mater Technol.* 2008 September 19;130(4):041010.
- [15] Zhang H, Li X, Qian W, Zhu J, Chen B, Yang J, et al. Characterization of mechanical properties of epoxy/nanohybrid composites by nanoindentation. *Nanotechnol Rev.* 2020;9(1):28–40.
- [16] Zhou Y, Wang Y, Fan M. Incorporation of tyre rubber into wood plastic composites to develop novel multifunctional composites: interface and bonding mechanisms. *Ind Crop Products.* 1 December 2019;141:111788.
- [17] Rao J, Zhou Y, Fan M. Revealing the interface structure and bonding mechanism of coupling agent treated WPC. *Polymers.* 2018;10(3):266.
- [18] Oliver WC, Pharr GM. An improved technique for determining hardness and elastic modulus using load and displacement sensing indentation experiments. *J Mater Res.* 1992;7(6):1564–83.
- [19] Zhou Y, Fan M, Lin L. Investigation of bulk and in situ mechanical properties of coupling agents treated wood plastic composites. *Polym Test.* 2017;4(58):292–9.
- [20] Bengtsson M, Gatenholm P, Oksman K. The effect of cross-linking on the properties of polyethylene/wood flour composites. *Compos Sci Technol.* 2005;65(10):1468–79.
- [21] Mohanty S, Verma SK, Nayak SK. Dynamic mechanical and thermal properties of MAPE treated jute/HDPE composites. *Compos Sci Technol.* 2006;66(3–4):538–47.
- [22] Mohanty S, Nayak SK. Interfacial, dynamic mechanical, and thermal fiber reinforced behavior of MAPE treated sisal fiber reinforced HDPE composites. *J Appl Polym Sci.* 2006;102(4):3306–15.
- [23] Ou R, Xie Y, Wolcott MP, Sui S, Wang Q. Morphology, mechanical properties, and dimensional stability of wood particle/high density polyethylene composites: effect of removal of wood cell wall composition. *Mater Des.* 2014;6(58):339–45.
- [24] López-Manchado MA, Biagitti J, Kenny JM. Comparative study of the effects of different fibers on the processing and properties of ternary composites based on PP-EPDM blends. *Polym Compos.* 2002;23(5):779–89.
- [25] Ratnam CT, Nasir M, Baharin A, Zaman K. Effect of electron-beam irradiation on poly(vinyl chloride)/epoxidized natural rubber blend: dynamic mechanical analysis. *Polym Int.* 2001;50(5):503–8.
- [26] Mehdi B, Mehdi T, Ghanbar E, Falk RH. Dynamic mechanical analysis of compatibilizer effect on the mechanical properties of wood flour – high-density polyethylene composites. *IJE Trans B: Appl.* 2004;17(1):95–104.
- [27] Thongsang S, Sombatsompop N. Effect of NaOH and Si69 treatments on the properties of fly ash/natural rubber composites*. *Polym Compos.* 2006;27(1):30–40.
- [28] Noriman NZ, Ismail H. Properties of styrene butadiene rubber (SBR)/recycled acrylonitrile butadiene rubber (NBR) blends: the effects of carbon black/silica (CB/Sil) hybrid filler and silane coupling agent, Si69. *J Appl Polym Sci.* 2012;124(1):19–27.
- [29] Ismail H, Shuhelmy S, Edyham MR. The effects of a silane coupling agent on curing characteristics and mechanical properties of bamboo fibre filled natural rubber composites. *Eur Polym J.* 2002;38(1):39–47.
- [30] Salimi D, Khorasani SN, Abadchi MR, Veshare SJ. Optimization of physico-mechanical properties of silica-filled NR/SBR compounds. *Adv Polym Technol.* 2009;28(4):224–32.
- [31] Ahmad I, Wong PY, Abdullah I. Effects of fiber composition and graft-copoly(ethylene/maleic anhydride) on thermoplastic natural rubber composites reinforced by aramid fiber. *Polym Compos.* 2006;27(4):395–401.
- [32] Konnerth J, Gindl W. Mechanical characterisation of wood-adhesive interphase cell walls by nanoindentation. *Holzforschung.* 2006;60(4):429–33.
- [33] Frihart CR. Adhesive bonding and performance testing of bonded wood products. *J ASTM Int.* 2005;2(7):1–10.
- [34] Gindl W, Schöberl T, Jeronimidis G. The interphase in phenol–formaldehyde and polymeric methylene di-phenyl-di-isocyanate glue lines in wood. *Int J Adhes Adhes.* 2004;24(4):279–86.